ELSEVIER

Journal of Nuclear Materials 241–243 (1997) 369–373

journal of nuclear materials

Divertor scaling laws for tokamaks

Peter J. Catto [a,*], D.A. Knoll [b], S.I. Krasheninnikov [c,d], J.W. Connor [e]

[a] *Massachusetts Institute of Technology, Plasma Fusion Center, NW16-236 167 Albany Street, Cambridge, MA 02139, USA*
[b] *Idaho National Engineering Laboratory, P.O. Box 1625, M.S. 3808, Idaho Falls, ID 83415, USA*
[c] *MIT, Plasma Fusion Center, NW16-234, Cambridge, MA, USA*
[d] *Kurchatov Institute, Moscow, Russia*
[e] *UKAEA Fusion (UKAEA / Euratom Fusion Association), Culham, Abingdon, Oxfordshire, OX14 3DB, UK*

Abstract

The breakdown of two body scaling laws is illustrated by using the two dimensional plasma code UEDGE coupled to an advanced Navier–Stokes neutrals transport package to model attached and detached regimes in a simplified geometry. Two body similarity scalings are used as benchmarks for runs retaining non-two body modifications due to the effects of (i) multi-step processes altering ionization and radiation via the excited states of atomic hydrogen and (ii) three body recombination. Preliminary investigations indicate that two body scaling interpretations of experimental data fail due to (i) multi-step processes when a significant region of the plasma exceeds a plasma density of 10^{19} m^{-3}, or (ii) three body recombination when there is a significant region in which the temperature is ≤ 1 eV while the plasma density is $\geq 10^{20}$ m^{-3}. These studies demonstrate that two body scaling arguments are often inappropriate in the divertor and the first results for alternate scalings are presented.

Keywords: Scaling law; Divertor plasma; Detached plasma; Atomic physics

1. Introduction

It is often difficult to identify the important underlying physical phenomena in edge plasmas because of the complexity of the edge region and the two dimensional (2D) transport codes developed for modeling it. This complexity has motivated efforts to determine key dimensionless parameters and scaling laws for edge plasmas from first principles. Lackner [1] applied similarity concepts [2] to tokamak edge plasmas by stressing the importance of atomic processes in the scrape off layer (SOL) and assuming that two body collisional interactions dominated. In Ref. [3] divertor scaling laws for a plasma (treated as a fluid) interacting with different neutrals models, including the boundary conditions, were analyzed in the two body collision approximation.

Divertor scaling law analyses have normally assumed that two body interactions dominate because ionization is typically viewed as a two body process and only recently has the important role that three body recombination plays in strongly detached operation begun to be recognized [4–7]. Recent work [8] noted, however, that two body scalings can fail even in the absence of recombination because multi-step atomic interactions involving the excited states of atomic hydrogen alter the ionization and radiation rates via the one body process of spontaneous decay. The violation of two body scaling due to multi-step transitions occurs if ionization of a significant population of excited atoms takes place before they are able to spontaneously decay to the ground state [9].

In the present work we extend the earlier studies to detached divertor operating regimes by also including the effect of three body recombination which improves detachment by reducing the plasma flux as it becomes significant. To gain insight into the role of recombination we again employ two body scaling predictions as a reference and to verify that our advanced neutral version of UEDGE

* Corresponding author. Tel.: +1-617 253 5825; fax: +1-617 253 5805; e-mail: catto@pfc.mit.edu.

PII S0022-3115(96)00531-4

[6–8] recovers two body scalings to a very high degree of accuracy in detached regimes. The Navier–Stokes advanced neutrals description incorporated into the version of UEDGE we employ accounts for neutral–neutral collisions [6], which are essential for reactor relevant divertor plasmas in order that the heat conduction coefficient of the neutral gas not be overestimated by orders of magnitude, as it would be if only neutral interactions with the ions were retained.

In practice, detached divertor regimes are normally achieved by reducing the heat flux into the hydrogen recycling region below some critical value by impurity radiation losses. Experiments [10–13] on most diverted tokamaks have demonstrated detached operation is characterized by the following: (1) high energy radiation losses from the SOL region; (2) low plasma temperature near the divertor plates; (3) strong decrease in the plasma particle and energy fluxes onto the target plates; and (4) strong plasma pressure drop along magnetic field lines in the divertor volume.

2. Background

The general form of the neutral kinetic equation retains neutral interactions with the neutrals, with the plasma, and with radiation and may be written as follows:

$$\vec{v}\cdot\nabla f_N(\vec{v},\vec{r},\vec{\alpha}) = C_{N,N} + C_{N,p} + C_{N,\hbar\omega}. \qquad (1)$$

In Eq. (1), $f_N(\vec{v},\vec{r},\vec{\alpha})$ is the neutral distribution function, $\vec{v}$ is the velocity, $\vec{r}$ is the spatial variable, and $\vec{\alpha}$ denotes all possible quantum states. We consider the simplest case of the transport of atomic hydrogen neutrals with parameters characteristic of a tokamak edge plasma. The interaction operators $C_{N,N}$ and $C_{N,p}$ describe neutral–neutral and neutral–plasma interactions, while the term $C_{N,\hbar\omega}$ accounts for effects involving radiation. Only two body elastic neutral–neutral collisions enter the term $C_{N,N}$, while non-two body interactions enter the other two interaction operators.

The neutral–plasma interaction term $C_{N,p}$ represents both two and three body interactions. The two body processes include elastic neutral–ion, neutral–electron, and charge exchange collisions; and electron (e) and ion (H^+) impact excitation ($n' > n$), de-excitation ($n' < n$), and ionization interactions:

$$H(n) + e \rightarrow H(n') + e,$$

$$H(n) + H^+ \rightarrow H(n') + H^+,$$

$$H(n) + e \rightarrow H^+ + 2e$$

and $$H(n) + H^+ \rightarrow 2H^+ + e,$$

where n is the principal quantum number. UEDGE neglects ion impact excitation, de-excitation, and ionization. The only non-two body process in $C_{N,p}$ is three body recombination

$$H^+ + 2e \rightarrow H(n) + e.$$

In general, the radiation term $C_{N,\hbar\omega}$ includes both one and two body interactions. The one body process is the spontaneous decay of excited states

$$H(n) \rightarrow H(n' < n) + h\nu.$$

Other processes that can enter $C_{N,\hbar\omega}$ are the two body processes of resonant absorption ($H(n) + h\nu \rightarrow H(n' > n)$) and induced emission ($H(n) + h\nu \rightarrow H(n' < n) + 2h\nu$) of radiation, and radiative ionization ($H(n) + h\nu \rightarrow H^+ + e$) and recombination ($H^+ + e \rightarrow H(n) + h\nu$).

Closure of the equations describing neutral transport requires a radiation transport description in the most interesting regimes of dense divertor operation since the plasma is optically thick [4,9]. In these regimes two body scaling is not recovered because radiation transport includes the effects of spectral line broadening due to micro-electric fields (a multi-body process) [14] as well as spontaneous emission. Often the plasma is assumed to be optically thin so that only spontaneous decay need be retained in $C_{N,\hbar\omega}$. The version of UEDGE we employ adopts the optically transparent plasma approximation and includes the coupling to a Navier–Stokes neutral transport package [6].

Even with the optically thin assumption, Eq. (1) contains one, two, and three body interaction terms. Two body scaling laws [1,3] for neutral transport in an optically transparent plasma can only be recovered if three body plasma recombination is unimportant, and either the spontaneous decay term is much smaller than other terms in Eq. (1) or the spontaneous decay of the excited neutral states occurs before they are able to have significant impact on other processes important in edge plasmas (e.g., ionization and/or recombination, or energy radiation losses). Roughly speaking, the effect of multi-step processes on the atomic hydrogen rate constants can only be neglected for plasma densities below 10^{19} m^{-3} in optically thin plasmas [9].

3. Method and results

The UEDGE calculations are performed in a rectangular geometry corresponding to the divertor region between the X-point and target. We impose a prescribed energy flux profile and zero particle flux condition on the upstream boundary, and complete plasma recycling at the target. We employ Alcator C-Mod edge plasma parameters ($B_{pol}/B = 0.06$, 25 cm poloidal distance between the X and strike points, and a 5 cm radial width) to perform the base case simulations. In the set of weakly detached runs of Figs. 1–4 the peak parallel energy flux and plasma pressure at the divertor entrance for the base case are taken to be 105 MW/m^2 and 800 Pa, respectively, and anomalous plasma particle and heat diffusivities of 0.5 m^2/s are

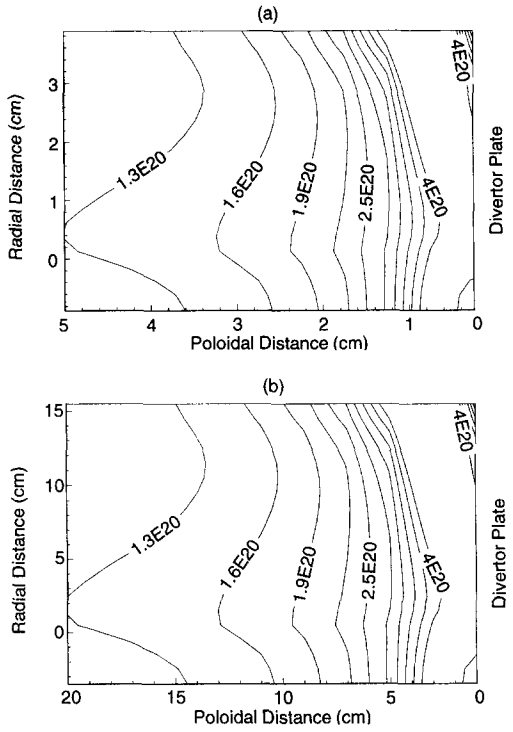

Fig. 1. (a) is a contour plot of the plasma density for the base case for the 5 cm nearest the target. (b) is a contour plot of the plasma density multiplied by four for the four times larger scaled case.

employed; resulting in a peak upstream plasma density and temperature of $\sim 7 \times 10^{19}$ m^{-3} and ~ 40 eV.

To benchmark the code against two body scalings, we first neglect recombination and use an alternate atomic hydrogen ionization rate model with no plasma density dependence. In this case the hydrogen radiation rate model is the same as that for ionization with a 13.6 eV energy loss per ionization. Next, two classes of non-two body runs are considered: one set without recombination and the other with. In both we employ an atomic hydrogen ionization rate constant model that retains the plasma density dependence due to multi-step processes. Multi-step processes are also retained in the hydrogen radiation plus ionization loss evaluation by using this same rate constant with a density and temperature dependent energy loss cost per ionization.

We first run a base two body case that is weakly detached. Its density contours are shown in Fig. 1(a) for the 5 cm in front of the target. Next a scaled two body detached simulation is performed. Two body scaling [1,3] requires that similar solutions be obtained when the product of the distribution function (that is, density, pressure, and heat flux) and all geometrical lengths are held fixed. Quadrupling all dimensions of our computational domain (including the grid spacing) and the anomalous transport coefficients [8], and reducing the upstream pressure and energy flux by a factor of four must give the same normalized solution. The scaled results for the density times four contours shown in Fig. 1(b), for the 20 cm in front of the plate, illustrate that exact two body similarity is obtained. This test of two body similarity provides an important benchmarking of the UEDGE code.

Next, we run the base, Fig. 2(a), and scaled, Fig. 2(b), cases with multi-step processes turned on in the atomic hydrogen ionization and radiation rates but without recombination. Notice that two body similarity is not satisfied (scaled densities are again multiplied by four). Two body similarity is violated because the effects of multi-step processes can only be neglected, roughly speaking, below about 10^{19} m^{-3} in optically thin plasmas [9], while even our lower density simulations exceed 10^{20} m^{-3} in some regions.

Finally, we run the base, Fig. 3(a), and scaled, Fig. 3(b), cases with recombination as well as multi-step effects on. Recombination is not playing a detectable role in the base case because detachment is relatively weak. In the scaled case the temperature at the plate is lower because the energy loss cost per ionization increases as multi-step processes become weaker at lower densities (thereby enhancing radiation losses more than ionization). Because the recombination rate is roughly $\propto N_e^3/T^{9/2}$, recombination

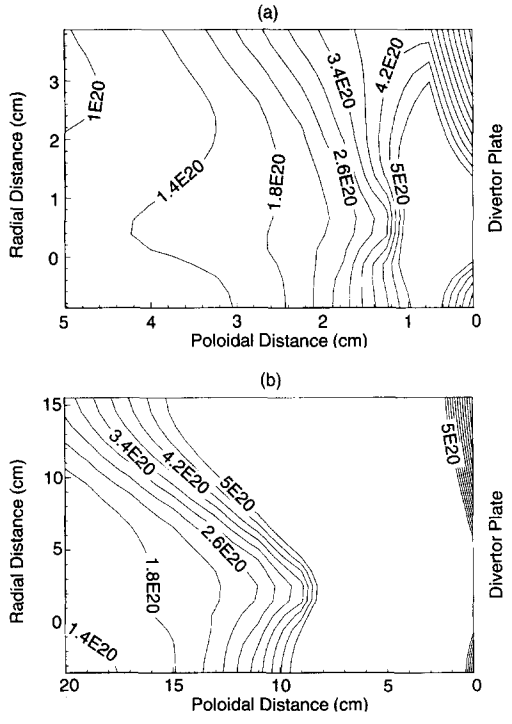

Fig. 2. (a, b) show the plasma density for the same cases as in Fig. 1(a) and (b) respectively, but with recombination off and multi-step processes turned on.

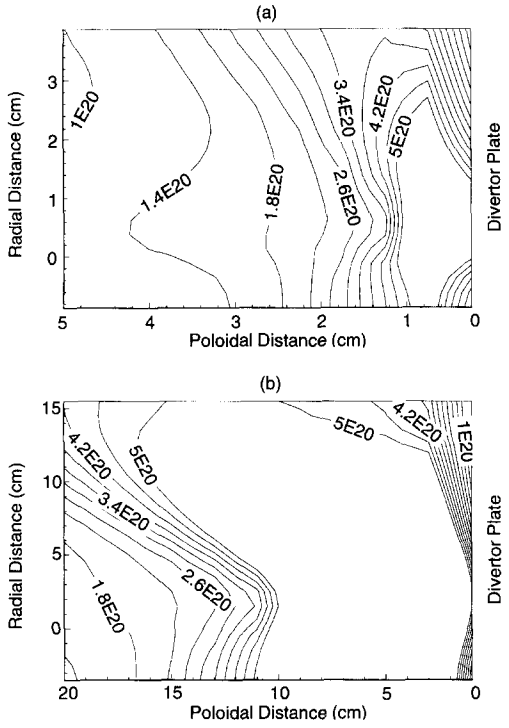

Fig. 3. (a, b) show the plasma density for the same cases as in Fig. 2Fig. 3 (a) and (b), but with both recombination and multi-step processes turned on.

begins to become significant due to the lower plasma temperature T near the target even though the plasma density N_e near the plate is also lower.

The violation of two body similarity is also apparent from the appropriately normalized heat fluxes onto the target (which include the energy released due to surface recombination), as indicated by Fig. 4. Scaled heat fluxes are multiplied by four to compare them with base cases. Comparing the curves, we see that for the higher, base case (lower, scaled case) plasma densities, multi-step processes result in a higher (lower) normalized target heat load. At higher (lower) densities fewer (more) excitations and decays occur prior to ionization, so the energy cost per ionization decreases (increases) while the ionization rate increases (decreases), with the competition resulting in a higher (lower) normalized heat flux to the target. The base curves in Fig. 4 are essentially the same since recombination remains negligible because the density is $\sim 10^{20}$ m^{-3} where the temperature is below 1 eV. However, for the scaled curves recombination reduces the target heat load substantially because there is a large region with the temperature below 1 eV and the density $\sim 10^{20}$ m^{-3}.

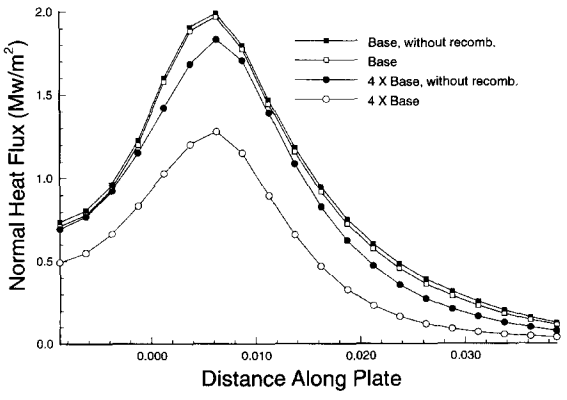

Fig. 4. The heat fluxes onto the target for the base cases of Fig. 2a and Fig. 3a are compared to four times the heat fluxes for the scaled cases of Fig. 2b and Fig. 3b.

4. Conclusions

The base and scaled runs of Figs. 1–4 illustrate the importance of non-two body effects in developing scaling laws and the usefulness of two body scaling for benchmarking complex edge codes. Two body scaling laws fail when multi-step processes become important in a significant region of the plasma (they enter when the plasma density $> 10^{19}$ m^{-3}); or when three body recombination becomes important in a significant region (it enters when the temperature is ≤ 1 eV while the plasma density is $\geq 10^{20}$ m^{-3}). In the absence of recombination, multi-step processes result in a higher (lower) density-normalized heat load at higher (lower) densities. Turning recombination on with a high density, low temperature region in front of the plates, results in a decrease in the heat load. To determine the optimum operating regime non-two body scalings need to be developed. For the model considered here we must supplement the usual two body divertor scaling parameters of the entering peak parallel energy flux at the X-point q_x normalized by the peak X-point plasma pressure p_x (q_x/p_x, in MW/m^2 Pa), collisionality ($p_x L$, with L the poloidal distance from the X-point to the target), and normalized diffusivity (D/L, with D the anomalous transport coefficient) with a separate p_x depen-

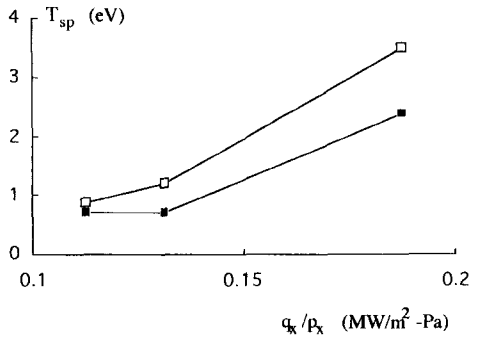

Fig. 5. Strike point temperature T_{sp} versus various q_x/p_x for the base case $p_x = 800$ Pa (upper curve, open squares) and scaled case $p_x = 200$ Pa (lower curve, shaded squares).

dence due to non-two body interactions. A plot of the strike point temperature T_{sp} versus three values of q_x/p_x for $p_x = 800$ Pa (base = upper curve) and $p_x = 200$ Pa (scaled = lower curve) results in the curves shown in Fig. 5 (which would be identical for two body scaling). For the constant collisionality ($p_x L =$ constant) scalings considered, Figs. 4 and 5 imply that larger machines have lower plate temperatures and normalized target heat loads, and can obtain detachment at lower upstream pressures. Note that $q_x/p_x \propto P/R =$ input power/major radius since $P \propto q_x Ra \propto q_x R/p_x$ and $p_x a =$ constant with a the minor radius.

Acknowledgements

Research supported by the USDOE under grant DE-FG02-91ER-54109 at MIT and contract DE-AC07-94ID13223 at INEL, and by the UK Department of Trade and Industry and Euratom at Culham.

References

[1] K. Lackner, Comments Plasma Phys. Controlled Fusion 15 (1994) 359.
[2] B.B. Kadomtsev, Sov. J. Plasma Phys. 1 (1975) 295; J.W. Connor and J.B. Taylor, Nucl. Fusion 17 (1977) 1047; B.B. Kadomtsev, Comments Plasma Phys. Controlled Fusion 13 (1989) 57.
[3] P.J. Catto, S.I. Krasheninnikov and J.W. Connor, Phys. Plasmas 3 (1996) 927.
[4] S.I. Krasheninnikov and A.Yu. Pigarov, Plasma Phys. Controlled Nucl. Fusion Res. (Infl. Atomic Energy Agency, Vienna, 1988) 3 (1986) 387.
[5] G. Porter et al., Phys. Plasmas 3 (1996) 1967.
[6] D.A. Knoll, P.R. McHugh, S.I. Krasheninnikov and D.J. Sigmar, Phys. Plasmas 3 (1996) 293.
[7] F. Wising, D.A. Knoll, S.I. Krasheninnikov, T.D. Rognlien and D.J. Sigmar, these Proceedings, p. 273.
[8] P.J. Catto, D.A. Knoll and S.I. Krasheninnikov, Phys. Plasmas 3 (1996) 3191.
[9] D.E. Post, J. Nucl. Mater. 220–222 (1995) 143.
[10] I.H. Hutchinson et al., Phys. Plasmas 1 (1994) 1511.
[11] G. Janeschitz et al., 19th Europ. Conf. on Controlled Fusion and Plasma Phys., Vol. 16C, Part II (Innsbruck, Austria, 1992) p. 727.
[12] T.W. Petrie et al., J. Nucl. Mater. 196–198 (1992) 848.
[13] V. Mertens et al., 20th Europ. Conf. on Controlled Fusion and Plasma Phys., Lisbon, Spain, 1993, Vol. 17C, Part I, p. 267.
[14] H.R. Griem, Spectral Line Broadening by Plasmas (Academic Press, New York, 1974).